

Article

# Voltammetric and Spectroscopic Investigation of Electrogenerated Oligo-Thiophenes: Effect of Substituents on the Energy-Gap Value

Maria I. Pilo <sup>\*</sup>, Elisabetta Masolo, Luca Maidich , Paola Manca, Gavino Sanna , Nadia Spano   
and Antonio Zucca 

Department of Chemical, Physical, Mathematical and Natural Sciences, University of Sassari, Via Vienna 2, 07100 Sassari, Italy

\* Correspondence: mpilo@uniss.it

**Featured Application:** Redox and optical features of thiophene-based oligomers and polymers make them appealing in several technological fields, including light-emitting diodes, solar cells, electrochromic and electroluminescent devices. In this context, the evaluation of the energy gap can give useful suggestions on the effect of substituents on the behavior of the oligothiophenes chain, and on the extension of the electron density delocalization.

**Abstract:** Oligothiophenes are especially appealing due to their promising applications in different fields, including photosensitive devices. In this context, anchoring a selected substituent on the main structure of the starting material can induce changes in redox and spectroscopic features, according to the nature of the substituent and its position on central or terminal rings. Here, an electrochemical and spectroscopic comparison between 2,2':5',2''-terthiophene (**2**), 5-Br-terthiophene (**3**) and 5-ethynyl-terthiophene (**5-ET**) is reported, aimed at elucidating the effect of the nature of the substituent on the energy gap value of the terthiophene skeleton. Furthermore, in order to understand the influence of a selected substituent in varying its position on the terthiophene backbone, **5-ET** is compared to the previously described 3'-ethynyl-terthiophene (**3'-ET**). Experimental results are confirmed by DFT calculations, showing a higher extension of the electron density in **5-ET** compared to **2** and **3**, as well as to **3'-ET**. In addition, as a consequence of the presence of the unsaturated fragment on the C-5-position, the energy gap value of poly-**5-ET** (the electrogenerated film from **5-ET**) appears significantly lower than poly-**2** and poly-**3**. Finally, the higher conjugation effect of a terminal acetylene fragment compared to a central one is confirmed by the energy gap values of poly-**5-ET** and poly-**3'-ET**.

**Keywords:** oligothiophenes; conducting polymers; electrochemical synthesis



**Citation:** Pilo, M.I.; Masolo, E.; Maidich, L.; Manca, P.; Sanna, G.; Spano, N.; Zucca, A. Voltammetric and Spectroscopic Investigation of Electrogenerated Oligo-Thiophenes: Effect of Substituents on the Energy-Gap Value. *Appl. Sci.* **2022**, *12*, 11714. <https://doi.org/10.3390/app122211714>

Academic Editor: Emiliano Principi

Received: 17 October 2022

Accepted: 16 November 2022

Published: 18 November 2022

**Publisher's Note:** MDPI stays neutral with regard to jurisdictional claims in published maps and institutional affiliations.



**Copyright:** © 2022 by the authors. Licensee MDPI, Basel, Switzerland. This article is an open access article distributed under the terms and conditions of the Creative Commons Attribution (CC BY) license (<https://creativecommons.org/licenses/by/4.0/>).

## 1. Introduction

Conducting polymers (CPs) are a well-known, wide class of compounds where the structural flexibility and the mechanical properties of “classical” polymers are coupled to the electronic and optical properties typical of inorganic semi-conductors. Since the Nobel Prize that was awarded to Heeger, McDiarmid, and Shirakawa in 2000, CPs have received a large attention from the scientific community due to their possible application in different technological fields such as sensors [1–6], photosensitive and electrochromic devices [7–13], rechargeable batteries [14–16], corrosion protection [17–19], and biomedicine [20,21]. In this context, polythiophenes (PTs) are especially appealing because of their structural versatility, as well as their environmental and thermal stability in the doped and undoped states, moderate band gap values, ease in p- and n-doping, and high conductivity [22]. CPs, including PTs, are often successfully achieved by electrochemical polymerization, with some interesting advantages to this methodology compared to the classical synthetic

approach. The electrochemical synthesis of a conducting polymer allows for obtaining a polymer film on an electrode surface, tuning the thickness by the deposition charge, and monitoring the growth process by electrochemical or spectroelectrochemical techniques. Furthermore, the CP-modified electrode surface can be directly used in some specific applications, as in the case of sensors. Additionally, the electro-generated polymer can be firstly characterized on the same electrode surface where it is grown [23]. The features of the film can be controlled through an appropriate selection of the experimental conditions, namely electrode material, monomer concentration, solvent and supporting electrolyte, temperature, pH (in case of aqueous solutions), and the electrochemical technique of deposition. From a general point of view, the electrical and optical properties of PTs are due to the extended charge delocalization along the polymer backbone as a consequence of the overlapping of the  $\pi$  orbital of the thiophene rings, which tend to be coplanar. On the other hand, the rigidity of the structure causes insolubility of unsubstituted PTs, making their chemical characterization difficult. The insertion of flexible chains as substituents on the polymer skeleton increases the solubility of PTs but produces a twisting in the structure, and consequent changes in the properties of the polymer [24]. Furthermore, the presence of substituents in the  $\beta$  position of the heterocyclic ring facilitates  $\alpha$ - $\alpha$  couplings rather than the  $\alpha$ - $\beta$ , leading mostly to stereoregular chains. In order to promote  $\alpha$ - $\alpha$  couplings, as well as to reduce the value of the potential in electrochemical polymerization of thiophenes, chemically synthesized oligomers can be used as starting materials [25,26]. A combination of all these aspects influences the mean effective conjugation length of the polymer chain and, consequently, its band gap energy and conductivity values. However, the effect of using monomers/oligomers as starting materials on the properties of the electrogenerated conducting polymers is not totally defined. In 1986, Roncali et al. [25] proved that polythiophenes obtained by mono-, bi- and ter-thiophene showed an increasing doping potential moving from poly (thiophene) to poly (terthiophene), suggesting a decrease of the mean conjugation length when increasing the number of heterocyclic rings in the relative oligomer. On the other hand, Zotti and Schiavon [26] reported that polythiophenes obtained from bi- and ter-thiophene showed comparable conductivity, whereas the polymer obtained by thiophene monomer showed lower conductivity values, maybe because of overoxidation processes that generate degradation phenomena. However, the lower oxidation potential of bi- and ter-thiophene, compared to thiophene as it is, allows to avoid overoxidation phenomena on the growing polymer. Therefore, these oligomers are often used in the electrochemical synthesis of thiophene polymers.

In this context, the functionalization of terthiophene (Figure 1) on the C-3' position is often adopted to assign new features to thiophene-based CPs.

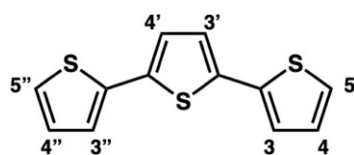


Figure 1. 2,2':5',2''-terthiophene.

The synthesis of terthiophene oligomers with N-chelating moieties, connected to the central thiophene ring through a saturated or an unsaturated tether, has been previously reported [22,27,28]. Such arrangements allow to combine the polymerizing ability of the terthiophene to the coordinating ability of the N-ligand towards metal ions, mixing the conducting properties of the organic framework to the electronic and optical properties of the metal center. The resulting metal-containing species can be included in the so-called "outer-sphere metallopolymers" group [29]. In particular, an unsaturated (ethynyl) spacer between the polymerizing and coordinating units instead of a saturated (methoxy) one leads to a higher extension of conjugation, evidenced by a lower energy gap value. On the other hand, 5-substituted terthiophenes are reported as building blocks in photo-sensitive arrangements [30,31]. As in the case of 3'-ethynyl-terthiophene, the analogue 5-ethynyl

derivative could be properly modified to achieve a molecule with a double function, that is, a polymerizing and a coordinating one. In this last case, the resulting metallopolymers could be defined as “inner-sphere metallopolymers” [29], with conducting, electronic, and optical performances higher than in the case of outer-sphere materials. In this context, a comparison between 3'-ethynyl- and 5-ethynyl-terthiophene could give useful suggestions to predict the optical and electrochemical behavior of new species, including such fragments as building block. Unlike 3'-ethynyl-terthiophene, the behavior of the 5-ethynyl- analogue has been reported only as a part of organic [31] or metallorganic [32,33] compounds, but its electrochemical characterization has not so far been reported to the best of our knowledge. Hence, with the aim of studying the influence of the position of an ethynyl substituent on the properties of the monomers and the resulting polymers, here we report a voltammetric and UV-Vis characterization of 5-ethynyl-terthiophene and poly (5-ethynyl-terthiophene), as well as a comparison of the corresponding 3'-ethynyl-terthiophene species. The experimental results are compared to calculated data by DFT-approach.

## 2. Materials and Methods

5-bromo-2,2'-bithiophene, 2-thienylboronic acid, tetrakis (triphenylphosphine) palladium (0) ([Pd(PPh<sub>3</sub>)<sub>4</sub>]), 1,1'-bis (diphenylphosphino) ferrocene dichloropalladium ([Pd(dppf)Cl<sub>2</sub>]), trimethylsilylacetylene (TMS), and N-bromo-succinimide (NBS) were from TCI Chemicals.

<sup>1</sup>H NMR spectra were recorded with a Varian VXR 300 spectrometer operating at 300.0 MHz. Chemical shifts are given in ppm relative to residual solvent signal [34].

UV-Vis spectra of the monomers were recorded in CH<sub>2</sub>Cl<sub>2</sub> or CH<sub>3</sub>CN solvent using a Hitachi U-2010 spectrophotometer. IR spectra were carried out with a JASCO FT/IR-489 Plus spectrophotometer using KBr disks in the range 4000–400 cm<sup>-1</sup>.

UV-Vis spectra of polymers were carried out on films electrodeposited on a ITO (indium-tin oxide) slide.

Electrochemical tests were performed with a AUTOLAB PGSTAT12 instrument, using the software GPES. The electrochemical synthesis and characterization were performed in a three-electrodes, single compartment cell using a Pt disk (2 mm diameter) as the working electrode, a graphite bar as the counter electrode, and Ag/AgCl equipped with a salt bridge containing the same solvent-supporting electrolyte system as the reference electrode. CH<sub>3</sub>CN or CH<sub>2</sub>Cl<sub>2</sub> (99.8%, packaged under nitrogen), and 0.1 M tetraethylammonium hexafluorophosphate (TEAPF<sub>6</sub>, puriss. electrochemical grade) were used as a solvent and supporting electrolyte, respectively. Before each experiment, the working electrode was polished with 1 and 0.3 μm alumina powder, then rinsed with distilled water in an ultrasonic bath. The monomer concentration in electrosynthesis and monomers characterizations was 2 × 10<sup>-3</sup> M. All the electrochemical experiments were performed under Ar atmosphere.

The energies of HOMO and LUMO were estimated by the voltammetric response according to Equations (1) and (2) [35]:

$$\text{HOMO} = -e(E_{\text{onset,ox}} + 4.71) \text{ (eV)} \quad (1)$$

$$\text{LUMO} = -e(E_{\text{onset,red}} + 4.71) \text{ (eV)} \quad (2)$$

where potential values are in Volts vs. Ag/AgCl and 4.71 is the potential (in Volts) of the redox couple Ag/AgCl versus vacuum, and taking into account that an electronvolt (eV) is defined as the energy gained by an electron moving along a potential of 1 V. The energy gap (E<sub>g</sub>) values (difference between LUMO and HOMO) were calculated from the electrochemical data (E<sub>g,ec</sub>), or from the UV-Vis spectra (E<sub>g,opt</sub>) according to Equation (3):

$$E_{g,\text{opt}} = 1239.81/\lambda_{\text{onset}} \quad (3)$$

where λ<sub>onset</sub> is the value of wavelength corresponding to 10% of maximum absorbance.

**DFT calculations.** DFT calculations were performed on PC GAMESS software [36], partially based on the GAMESS (US) source code [37] using the PBE0 functional [38] with

the basis set split-valence according to reference [39]. Concerning iodide, the corresponding pseudo-potential removing 28 core-electrons was adopted.

Harmonic analysis at PBE0/def2-SVP level was carried out on the equilibrium geometries of the substituted 2,2':5',2''-terthiophenes to confirm the nature of the minimum (i.e., the absence of imaginary frequencies) on the PES (Potential Energy Surface). The first 30 excited states were calculated from the equilibrium geometries at gas phase using the TD-DFT approach [40]. The resulting files were elaborated under Avogadro [41] and Gabedit software [42], released under GNU license.

*Synthesis of 2,2':5',2''-terthiophene (2).* 5-bromo-2,2'-bithiophene (**1**, 0.5827 g, 2.378 mmol) and [Pd(PPh<sub>3</sub>)<sub>4</sub>] (0.1644 g, 0.142 mmol) were dissolved in DME (15 mL). After 10 min, 2-thienylboronic acid (0.4473 g, 4.276 mmol) and 1 M NaHCO<sub>3</sub> aqueous solution (5.2 mL) were added. The reaction mixture was stirred at reflux temperature for 30 min and monitored by TLC (petroleum ether/dichloromethane 9/1 as eluent) until **1** disappeared, then cooled at room temperature and filtered. H<sub>2</sub>O (20 mL) was added to the residue, the organic phase was extracted with diethyl ether (3 × 30 mL) and washed with water (90 mL). Finally, the solution was treated with MgSO<sub>4</sub> and filtered, and the solvent was evaporated under reduced pressure. The crude product was purified by column chromatography on silica, using petroleum ether/dichloromethane 9/1 as eluent, to give 2,2':5',2''-terthiophene (**2**, 0.5612 g, 2.259 mmol, yield 95%). <sup>1</sup>H NMR (CD<sub>2</sub>Cl<sub>2</sub>, ppm), δ<sub>H</sub>: 7.29 (dd, 2H, H<sub>5</sub> + H<sub>5''</sub>, <sup>3</sup>J = 5.1 Hz, <sup>4</sup>J = 1.0 Hz); 7.23 (dd, 2H, H<sub>3</sub> + H<sub>3''</sub>, <sup>3</sup>J = 3.6 Hz, <sup>4</sup>J = 1.0 Hz); 7.14 (s, 2H, H<sub>3'</sub> + H<sub>4'</sub>); 7.07 (dd, 2H, H<sub>4</sub> + H<sub>4''</sub>, <sup>3</sup>J = 5.1 Hz, <sup>4</sup>J = 3.6 Hz).

*Synthesis of 5-bromo-2,2':5',2''-terthiophene (3).* NBS (0.3187 g, 1.790 mmol) was added drop by drop to a solution of terthiophene (**2**, 0.4922 g, 1.982 mmol) in DMF (6 mL). The additions were performed out of light, during 6 h, at −20 °C, under stirring. At the end of the additions, the reaction mixture was taken to room temperature, then the reaction was let to proceed further for 24 h. Finally, the mixture was poured into iced water (60 mL), and extraction with CH<sub>2</sub>Cl<sub>2</sub> was performed. The organic phase was washed with H<sub>2</sub>O, treated with MgSO<sub>4</sub> and filtered, and the solvent was evaporated under reduced pressure. The crude product was crystallized with hexane to give **3** (0.5107 g, 1.560 mmol), with 79% yield. <sup>1</sup>H NMR (CD<sub>2</sub>Cl<sub>2</sub>, ppm), δ<sub>H</sub>: 7.30 (dd, 1H, H<sub>5''</sub>, <sup>3</sup>J = 5.1 Hz, <sup>4</sup>J = 1.0 Hz); 7.23 (dd, 1H, H<sub>3''</sub>, <sup>3</sup>J = 3.6 Hz, <sup>4</sup>J = 1.0 Hz); 7.13 (d, 1H, H<sub>4'</sub>, <sup>3</sup>J = 3.8 Hz); 7.08 (d, 1H, H<sub>3'</sub>, <sup>3</sup>J = 3.8 Hz); 7.07 (dd, H<sub>4''</sub>, <sup>3</sup>J = 5.1 Hz, <sup>4</sup>J = 3.6 Hz); 7.04 (d, 1H, H<sub>4</sub>, <sup>3</sup>J = 3.9 Hz); 6.98 (d, 1H, H<sub>3</sub>, <sup>3</sup>J = 3.9 Hz).

*Synthesis of 5-(3-hydroxy-3-butyl-1-ynyl)-2,2':5',2''-terthiophene (4).* 5-bromo-2,2':5',2''-terthiophene (**3**, 0.2311 g, 0.707 mmol), [Pd(dppf)Cl<sub>2</sub>] (0.0057 g, 0.007 mmol) and CuI (0.0042 g, 0.022 mmol) were dissolved in diisopropylamine (5 mL), and 2-methyl-3-butyn-2-ol (0.0663 g, 0.076 mL, 0.788 mmol) was added. The mixture was heated at reflux temperature, with the initial yellow color turning to brown. The reaction was monitored by TLC (eluent: petroleum ether/ethyl acetate 5/1) for 24 h, until the substrate **3** disappeared. The mixture was cooled to room temperature, and CH<sub>2</sub>Cl<sub>2</sub> (25 mL) was added. The solution was washed with a saturated NaHCO<sub>3</sub> aqueous solution (25 mL) and H<sub>2</sub>O (25 mL), dehydrated with MgSO<sub>4</sub> and filtered, and the solvent was evaporated under vacuum. The crude product was purified by column chromatography on silica (petroleum ether/ethyl acetate 5/1 as eluent) to give **4** (0.1568 g, 0.474 mmol, yield 68%). <sup>1</sup>H NMR (CD<sub>2</sub>Cl<sub>2</sub>, ppm), δ<sub>H</sub>: 7.30 (dd, 1H, H<sub>5''</sub>, <sup>3</sup>J = 5.1 Hz, <sup>4</sup>J = 1.0 Hz); 7.24 (dd, 1H, H<sub>3''</sub>, <sup>3</sup>J = 3.6 Hz, <sup>4</sup>J = 1.0 Hz); 7.13 (d, 1H, partially overlapped, <sup>3</sup>J = 3.6 Hz); 7.07 (dd, 1H, H<sub>4'</sub>, J = 5.1, 3.6 Hz); 7.07 (d, 1H, J = 3.6 Hz); 2.17 (s, 1H, OH); 1.62 (s, 6H, CH<sub>3</sub>). IR (KBr, cm<sup>−1</sup>): 3342 (OH), 2203 (C≡C).

*Synthesis of 5-ethynyl-2,2':5',2''-terthiophene (5-ET).* 5-(3-hydroxy-3-methylbutyn-1-yl)-2,2':5',2''-terthiophene (**4**, 0.2654 g, 0.803 mmol) was dissolved in toluene/methanol 1/1 (previously deoxygenated), and a large excess of KOH was added (KOH/substrate 10/1). The reaction mixture was stirred at reflux temperature and monitored by TLC (eluent: petroleum ether/ethyl acetate 5/1) for 24 h, until the substrate disappeared. The mixture was cooled at room temperature and the solvent was concentrated to a small volume. Then, water (50 mL) was added, and the organic phase was extracted with CH<sub>2</sub>Cl<sub>2</sub> (3 × 50 mL), washed with a saturated NH<sub>4</sub>Cl aqueous solution (200 mL), treated with MgSO<sub>4</sub> and

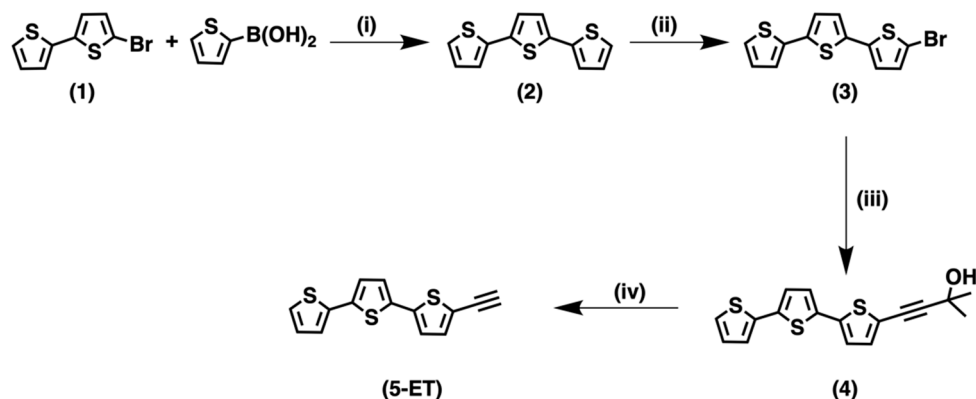
filtered. The solution was evaporated to dryness, and the crude residue was purified by column chromatography on silica, using petroleum ether/ethyl acetate 5/1 as eluent. The compound **5-ET** was obtained (0.1845 g, 0.671 mmol, 84% yield) as a brown-reddish powder.  $^1\text{H NMR}$  ( $\text{CD}_2\text{Cl}_2$ , ppm),  $\delta_{\text{H}}$ : 7.30 (dd, 1H,  $\text{H}_{5''}$ ,  $^3\text{J} = 5.1$  Hz,  $^4\text{J} = 1.0$  Hz); 7.24 (dd, 1H,  $\text{H}_{3''}$ ,  $^3\text{J} = 3.6$  Hz,  $^4\text{J} = 1.0$  Hz); 7.23 (d, 1H,  $\text{J} = 3.6$  Hz); 7.15 (AB system,  $J_{\text{AB}} = 3.6$  Hz); 7.14 (AB system,  $J_{\text{AB}} = 3.6$  Hz); 7.09 ÷ 7.06 (m, 2H). IR (KBr,  $\text{cm}^{-1}$ ): 3276 (C≡C-H), 2094 (C≡C).

### 3. Results and Discussion

#### 3.1. Synthesis

The synthesis of 5-ethynyl-2,2':5',2''-terthiophene has been reported [31] as a combination of Stille and Sonogashira–Hagihara couplings. In this approach, 2,2':5',2''-terthiophene obtained by the reaction of 2,5-dibromothiophene with 2-(tributylstannyl)thiophene reacts with NBS to give the bromo-substituted derivative. The coupling reaction between the halo-thiophene and trimethylsilylacetylene (TMS) provides the TMS-ethynyl-terthiophene that is finally deprotected, leading to the ethynyl-derivative.

As an alternative, the synthetic route reported here can be successfully adopted. According to previous results [22], the synthesis of the ethynyl-terthiophene derivative **5-ET** (Scheme 1) involves a Sonogashira–Hagihara coupling reaction between the corresponding Br-derivative (**3**) and 2-methyl-3-butyn-2-ol, followed by treatment with KOH. The synthesis of **3** was first attempted using a classical Suzuki-type coupling between the 5-bromo-2,2'-dithiophene **1** and 5-bromo-2-thiopheneboronic acid, but it resulted in quite low yields (about 20%), ascribed to homo-coupling reactions of the bromo boronic acid. For this reason, 2-thienylboronic acid was employed instead of 5-bromo-2-thiopheneboronic acid, and its coupling with the Br-derivative **1** allowed to obtain the unsubstituted terthiophene **2** with very good yields (95%). Then, **2** underwent a selective bromination on the C-5 by reacting with NBS [43], and **3** was obtained with a significative increase in yields (75% on the whole). The reaction of the halo-thiophene **3** with 2-methyl-3-butyn-2-ol as the ethynyl synthon gave the intermediate product **4**. Finally, the deprotection of **4** with KOH allowed to obtain the target product **5-ET** in good yields (84%).



**Scheme 1.** Synthetic route for 5-ethynyl-terthiophene **5-ET**. (i)  $[\text{Pd}(\text{PPh}_3)_4]$ , DME, 1 M  $\text{NaHCO}_3$ ; (ii) NBS; (iii)  $[\text{Pd}(\text{dppf})\text{Cl}_2]$ , CuI, diisopropylamine, 2-methyl-3-butyn-2-ol; (iv) KOH, toluene/methanol 1/1.

#### 3.2. Characterization of Monomers

The electrochemical behavior of 2,2':5',2''-terthiophene (**2**), 5-bromo-2,2':5',2''-terthiophene (**3**), and 5-ethynyl-2,2':5',2''-terthiophene (**5-ET**) was investigated by cyclic voltammetry both in  $\text{CH}_2\text{Cl}_2$  and in  $\text{CH}_3\text{CN}$  as solvent, using 0.1 M  $\text{TEAPF}_6$  as the supporting electrolyte.

The cyclic voltammetry response of **2** in  $\text{CH}_2\text{Cl}_2$  (Figure 2a) shows a two-step anodic process, located at +1.13 V and at +1.18 V, with an associated process in the backward scan at +0.64 V. Both the second anodic process and the backward one evidence a sharp shape, suggesting adsorbing/desorbing phenomena on the electrode surface, according to investigations in different experimental conditions reported previously [25,44].

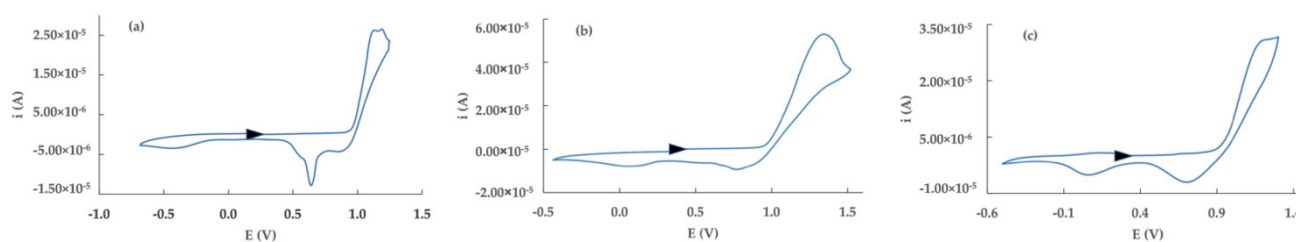


**Figure 2.** Cyclic voltammety responses of 2,2':5',2''-terthiophene (a), 5-Br-2,2':5',2''-terthiophene (b), and 5-ethynyl-2,2':5',2''-terthiophene (c) in  $\text{CH}_2\text{Cl}_2/0.1 \text{ M TEAPF}_6$ , potential scan rate: 100 mV/s. The black arrow indicates the starting potential and the scan direction.

Using  $\text{CH}_3\text{CN}$  as solvent in electrochemical investigations, a similar behavior is observed, with a double anodic system at lower potential values than in  $\text{CH}_2\text{Cl}_2$  (+1.05 and +1.09 V) and an associated backward peak (+0.82 V), the shape of the more anodic peak being reasonably attributed to the occurrence of absorptions (and corresponding desorptions) of oligomeric species on the electrode surface.

The presence of an electron-withdrawing -Br substituent on the C-5 position (compound **3**) causes a shift of the process towards more anodic values, both in  $\text{CH}_2\text{Cl}_2$  and on  $\text{CH}_3\text{CN}$  solvents. In particular, an anodic peak at +1.21 V (with an associated backward process at about +0.7 V), followed by a shoulder at 1.35 V is observed in  $\text{CH}_2\text{Cl}_2$  (Figure 2b). The voltammetric response in  $\text{CH}_3\text{CN}$  again shows two anodic processes (+1.13 and +1.23 V, respectively), where the second one increases in current intensity at subsequent scans.

The behavior of compound **5-ET**, where an ethynyl substituent is present in place of -Br, evidences a single anodic process at +1.15 V, with a backward associated signal at +0.73 V in  $\text{CH}_2\text{Cl}_2$  (Figure 2c). Changing the solvent to  $\text{CH}_3\text{CN}$ , an anodic process at +1.12 V is observed.

Electrochemical data of **2**, **3**, and **5-ET** are reported in Table 1, as well as 3'-ethynyl-2,2':5',2''-terthiophene (**3'-ET**, [22]) as a comparison, where the ethynyl substituent is on the central ring of the terthiophene structure rather than on a peripheral ring. HOMO values were referred to the  $\text{CH}_3\text{CN}$  solutions according to the analogous evaluation on the corresponding polymer species (Section 3.3).

**Table 1.** Electrochemical data of the terthiophene derivatives in  $\text{CH}_3\text{CN}/0.1 \text{ M TEAPF}_6$  and  $\text{CH}_2\text{Cl}_2/0.1 \text{ M TEAPF}_6$  solvent system.

| Compound                                 | $E_{\text{ox}}$ (V)                              |  | $E_{\text{ox,onset}}$ (V)                        |  | HOMO (eV) |
|--|--|--|--|--|-----------|
|  | $\text{CH}_2\text{Cl}_2/\text{TEAPF}_6$<br>0.1 M | $\text{CH}_3\text{CN}/\text{TEAPF}_6$<br>0.1 M | $\text{CH}_2\text{Cl}_2/\text{TEAPF}_6$<br>0.1 M | $\text{CH}_3\text{CN}/\text{TEAPF}_6$<br>0.1 M |           |
| 2,2':5',2''-terthiophene ( <b>2</b> )    | 1.13   | 1.05   | 0.97   | 0.95   | -5.66     |
| 5-Br-terthiophene ( <b>3</b> )           | 1.21   | 1.13   | 0.99   | 0.92   | -5.63     |
| 5-ethynyl-terthiophene ( <b>5-ET</b> )   | 1.15   | 1.12   | 0.93   | 0.91   | -5.62     |
| 3'-ethynyl-terthiophene ( <b>3'-ET</b> ) | 1.26   | 1.19   | 1.00   | 1.01   | -5.72     |

Potential values referred to Ag/AgCl. HOMO values referred to electrochemical responses in  $\text{CH}_3\text{CN}/0.1 \text{ M TEAPF}_6$ .

Table 1 evidences that an ethynyl substituent on the central ring makes the terthiophene structure more stable, whereas (Br- or ethynyl-) functionalization on the external ring does not meaningfully influence the voltammetric parameters and the corresponding HOMO values.

Compounds **2**, **3**, and **5-ET** were also investigated by UV-Vis spectroscopy, both in  $\text{CH}_2\text{Cl}_2$  and  $\text{CH}_3\text{CN}$ , and spectroscopic data were again compared to **3'-ET**. In all cases,  $\lambda_{\text{max}}$  values are always in the range 340–390 nm, and are ascribed to  $\pi-\pi^*$  transitions on the terthiophene [44,45], as confirmed by theoretical calculations (Table 2).

**Table 2.** Experimental  $\lambda_{\max}$  and  $E_g$  values compared to calculated values.

|                                 | $\lambda_{\max}$ (nm)           |                    |            | $E_{g,opt}$ (eV)                |                    |            |
|---------------------------------|---------------------------------|--------------------|------------|---------------------------------|--------------------|------------|
|                                 | CH <sub>2</sub> Cl <sub>2</sub> | CH <sub>3</sub> CN | Calculated | CH <sub>2</sub> Cl <sub>2</sub> | CH <sub>3</sub> CN | Calculated |
| 2,2':5':2''-terthiophene (2)    | 355                             | 358                | 364        | 3.10                            | 3.10               | 3.41       |
| 5-Br-terthiophene (3)           | 359                             | 359                | 374        | 3.04                            | 3.04               | 3.32       |
| 5-ethynyl-terthiophene (5-ET)   | 383                             | 379                | 388        | 2.88                            | 2.88               | 3.20       |
| 3'-ethynyl-terthiophene (3'-ET) | 352                             | 348                | 375        | 2.90                            | 2.95               | 3.31       |

The analysis of UV-Vis data suggests that the presence of -Br as a substituent on the C-5 atom of the terthiophene skeleton slightly affects the maximum absorbance wavelength, whereas an -ethynyl fragment on the same position of the ring results in a red shift in the  $\lambda_{\max}$  value, as well as a decrease in the  $E_g$  value. Furthermore, the comparison between 3'-ET and 5-ET suggests a slight lowering in  $E_g$  when the ethynyl substituent is in a peripheral position instead of on the central thiophene ring.

Experimental results were compared with theoretical calculations using the TD-DFT approach. Initially, a level RHF/STO-3G was tested to obtain an equilibrium geometry of the reference molecules that is the quaterthiophene [46]. Then, different functional/basis set couples were adopted and compared, as reported in Table 3. According to such a preliminary study, PBE0 functional with split-valence (def2-SVP) basis set shows the strongest agreement with the proposed structure, although the time required is quite long. Therefore, the PBE0/def2-SVP level was selected to calculate the singlet excited states.

**Table 3.** Computing time and percent average error (AE%) at different functionals and basis sets.

|          |             | PBE96 | OLYP  | B3LYP5 | B3PW91 | BHLYP | O3LYP5 | PBE0  |
|----------|-------------|-------|-------|--------|--------|-------|--------|-------|
| 3-21G    | Time (min)  | 85.6  | 123.8 | 94.9   | 100.2  | 91.1  | 99.1   | 82.9  |
|          | % AE (dist) | 2.65  | 2.49  | 2.31   | 2.02   | 1.91  | 1.76   | 1.85  |
|          | % AE (ang)  | 3.06  | 21.24 | 3.47   | 3.63   | 4.69  | 3.46   | 1.68  |
|          | % AE (all)  | 2.70  | 4.83  | 2.45   | 2.22   | 2.26  | 1.97   | 1.83  |
| 6-31G    | Time (min)  | 150.2 | 167.1 | 113.3  | 166.1  | 137.4 | 113.9  | 148.3 |
|          | % AE (dist) | 2.63  | 2.49  | 2.33   | 2.01   | 1.70  | 1.77   | 1.87  |
|          | % AE (ang)  | 1.74  | 15.22 | 4.63   | 5.95   | 5.84  | 4.75   | 3.85  |
|          | % AE (all)  | 2.52  | 4.08  | 2.61   | 2.50   | 2.22  | 2.14   | 2.12  |
| MC       | Time (min)  | 269.4 | 392   | 360.9  | 348.2  | 255.9 | 311.9  | 320.6 |
|          | % AE (dist) | 2.54  | 2.37  | 2.23   | 1.89   | 1.70  | 1.63   | 2.13  |
|          | % AE (ang)  | 4.78  | 20.95 | 8.76   | 10.09  | 9.15  | 8.56   | 6.57  |
|          | % AE (all)  | 2.82  | 4.69  | 3.05   | 2.92   | 2.63  | 2.49   | 2.69  |
| def2-SVP | Time (min)  | 445.9 | 476.2 | 382    | 435.3  | 523.9 | 455.4  | 470.6 |
|          | % AE (dist) | 1.28  | 1.14  | 1.01   | 0.72   | 0.34  | 0.70   | 0.63  |
|          | % AE (ang)  | 5.53  | 12.93 | 5.19   | 6.67   | 7.69  | 5.41   | 4.77  |
|          | % AE (all)  | 1.81  | 2.62  | 1.54   | 1.47   | 1.26  | 1.29   | 1.15  |

% AE: percent average error.

The second step was the choice of the proper structure of terthiophene for the relative position of heteroatoms (i.e., *cis-cis*, *cis-trans*, or *trans-trans*). From a general point of view, the structure of 2,2':5',2''-terthiophene has a conformational variability due to the free rotation of aromatic rings. For this reason, a tridimensional map has been calculated to observe the changing energies as a function of dihedral angles S-C-C-S in 2,2':5',2''-terthiophene (Figure 3). The map evidences a symmetric behavior with respect to the diagonal, suggesting an equivalence of the external aromatic rings. Moreover, the *trans-trans* configuration (with 180° dihedral angles) shows the lowest energy. Hence, although the situation in a solution phase is certainly more dynamic, the *trans-trans* configuration was selected for the optimizations adopted here.

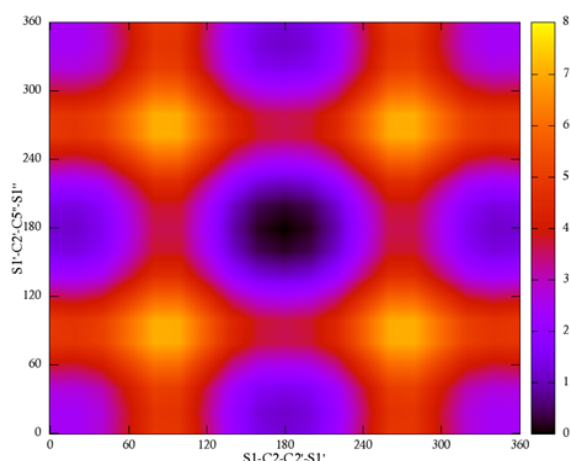


**Figure 3.** Energy surfaces as function of dihedral angles in 2,2':5',2''-terthiophene.

On these bases, the singlet excited states were calculated (Table 2) evidencing that all  $\lambda_{\max}$  values are in a narrow range (360–390 nm), being ascribable to  $\pi$ - $\pi^*$  transitions on the common terthiophene skeleton of the investigated species. Experimental and theoretical  $\lambda_{\max}$  values are in good agreement, as well as  $E_{g,\text{opt}}$  values, showing a 15% maximum difference between the calculated and experimental data. The red-shift in  $\lambda_{\max}$  and the corresponding lowering in  $E_{g,\text{opt}}$  argue a more extended conjugation in the terthiophene framework, due to the presence of an unsaturated fragment on the C-5 atom instead of on the C-3' position.

### 3.3. Electrochemical Polymerization and Polymer Characterization

Electrochemical polymerization of **2**, **3**, and **5-ET** was performed on a Pt disk as a working electrode by cyclic voltammetry (Figure 4), as well as, when successful, by chronoamperometry on a  $2 \times 10^{-3}$  M solution of each monomer in  $\text{CH}_2\text{Cl}_2/\text{TEAPF}_6$ .

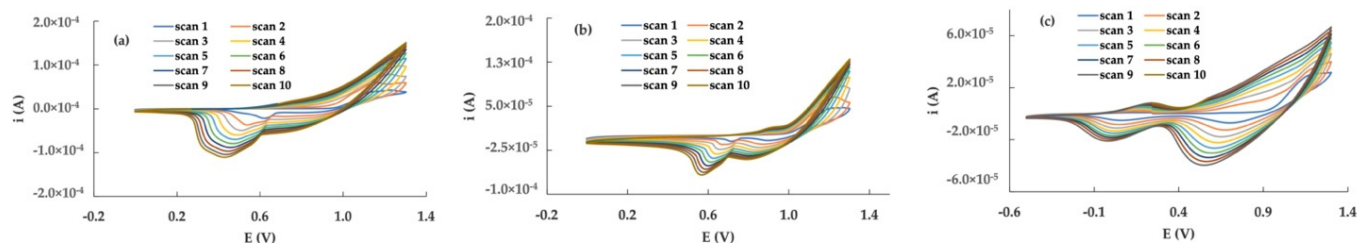


**Figure 4.** Cyclic voltammetry polymerization of **2** (a), **3** (b) and **5-ET** (c) on a Pt disk electrode in  $\text{CH}_2\text{Cl}_2/\text{TEAPF}_6$  0.1 M solvent system. Potential scan rate:  $100 \text{ mV s}^{-1}$ .

The potentiodynamic polymerization of terthiophene **2** by cycling the potential between 0 and 1.3 V evidences an increase in the current intensity when increasing the scan number. After 10 scans, a homogeneous deep-red polymer film was observed on the electrode surface.

A film of poly-**2** obtained by potentiostatic polymerization proved to be scarcely stable on the electrode surface, maybe due to the absorption/desorption processes mentioned in the previous section, as well as to a possible partial solubility of low-molecular-weight oligomer species.

The polymerization behavior of the Br-derivative **3** was similar to the unsubstituted terthiophene **2**, and a red polymer film of poly-**3** was obtained only by cyclic voltammetry, whereas the potentiodynamic polymerization was unsuccessful.

Lastly, the polymer form of 5-ethynyl-terthiophene (poly-**5-ET**) was initially obtained by cyclic voltammetry, scanning the potential from 0 and +1.25 V for 10 cycles. The potentiostatic approach was also successful in the polymerization of **5-ET**, being performed

at +1.12 V for 300 s, then neutralizing the film at 0 V for 60 s. In both cases, a stable brown-red film of poly-5-ET formed on the electrode surface.

To compare the electrochemical behavior of the polymer species here reported and poly-3'-ET [22], the voltammetric characterization of poly-2, poly-3 and poly-5-ET was performed in CH<sub>3</sub>CN/TEAPF<sub>6</sub> 0.1 M solution (Figure 5 and Table 4).

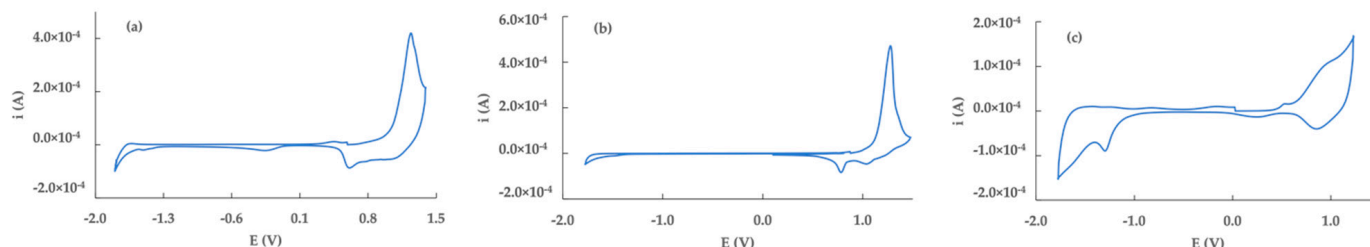


**Figure 5.** Cyclic voltammetry characterization of poly-2 (a), poly-3 (b) and poly-5-ET (c) in CH<sub>3</sub>CN/TEAPF<sub>6</sub> 0.1 M solution.

**Table 4.** Voltammetric data in CH<sub>3</sub>CN/TEAPF<sub>6</sub> 0.1 M and UV-Vis data of the polymer films.

|            | $E_{ox}$ (V) | $E_{rid}$ (V) | HOMO (eV) | LUMO (eV) | $E_{g,ec}$ (eV) | $E_{g,opt}$ (eV) |
|------------|--------------|---------------|-----------|-----------|-----------------|------------------|
| Poly-2     | 1.24         | −1.44         | −5.68     | −3.34     | 2.34            | 2.08             |
| Poly-3     | 1.28         | −1.48         | −5.81     | −3.35     | 2.46            | 2.21             |
| Poly-5-ET  | 0.93         | −1.68         | −5.37     | −3.63     | 1.74            | 1.89             |
| Poly-3'-ET | 1.05         | −1.73         | −5.47     | −3.40     | 2.07            | 2.06             |

The voltammetric response of poly-2 shows a doping/de-doping process at +1.26/0.57 V. The sharp shape of the anodic peak, quite unusual for a conducting polymer, is commonly ascribed to a narrow distribution of molecular weights along the polymer chains, leading to a harder oxidation process and to less conductive polymers [25]. On the following scans, the doping peak shifts to +1.1 V and becomes broader, suggesting a rearrangement of the polymer chains with different internal interactions.

The voltammetric behavior of poly-3 is similar to poly-2, showing a sharp doping at 1.24 V, with a double-step de-doping at +1.03 V and +0.80 V. In the case of the polymer form of Br-terthiophene, besides the narrow molecular weight distribution (attributed to the high conjugation of terthiophene monomer), the C-5 position is not available to the growth of the polymer chain due to the presence of -Br, hence reasonably only dimer species are formed. Both poly-2 and poly-3 show a cathodic process at −1.44 and −1.48 V, respectively, associated to the n-doping process on the polymer chain.

The voltammetric response of poly-5-ET evidences a significant lowering in the potential value of the doping/de-doping process, that appears at +1.05/+0.87 V. Furthermore, a pre-peak at +0.5 V is visible, maybe due to charge trapping phenomena [22]. The cathodic scan shows a sharp peak at −1.39 V and a second, broad at −1.68 V, suggesting the presence of charge trapping processes also in the negative section of the potential window.

UV-Vis characterization of neutral polymers (Table 4 and Figure 6) was performed on films grown on ITO as a working electrode. The spectra of poly-2 and poly-3 show three broad absorption bands between 600 and 450 nm ascribed to short-chain oligomers, and a transition around 360 nm due to the unreacted monomer. Hence, UV-Vis spectra of the polymer species deriving from unsubstituted and Br-substituted terthiophene confirm the hypothesis from the electrochemical data about the low efficiency of the polymerization process giving only low-molecular-weight species.

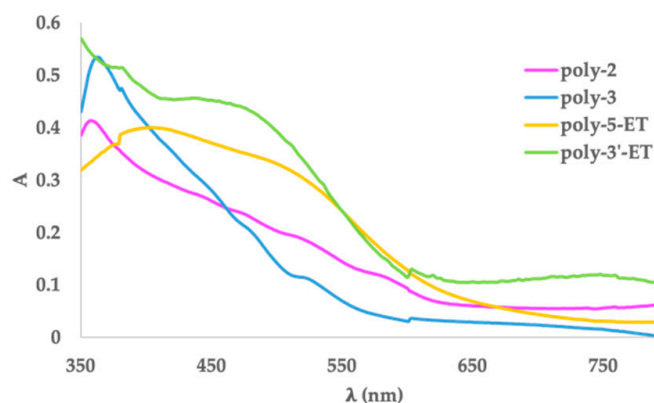


**Figure 6.** UV-Vis spectra of poly-2, poly-3, poly-5-ET and poly-3'-ET on ITO.

On the other side, the spectra of poly-5-ET and poly-3'-ET [22] do not evidence the presence of unpolymerized monomer, showing a broad absorption band over 400 nm.  $E_{g,opt}$  values were calculated from the onset wavelength. They are in good qualitative agreement with the corresponding values from the electrochemical investigation (Table 4). For all polymers, both electrochemical and spectroscopic  $E_g$  values are lower than the relevant monomers. Furthermore, the lowering of the  $E_g$  value from poly-2 (unsubstituted poly-terthiophene) to poly-3'-ET (ethynyl substituent on the central ring) looks smaller than to poly-5-ET (ethynyl on a peripheral ring). Such a difference suggests some comments on the effect of the ethynyl fragment depending on the position (central or external ring, respectively) where it is anchored on the relevant terthiophene monomer. A plausible reason for this behavior can be found according to the proposed coupling route for poly-3'-ET and for poly-5-ET in Figure 7. In particular, an unsaturated function on the central heterocycle ring (3'-ET) seems to be scarcely influencing the growing mechanism of the polymer chain. This feature can be reasonably attributed to  $\alpha$ - $\alpha$  couplings between external thiophene rings of two different terthiophene units, not directly involving the ethynyl substituent on C-3', which appears outside of the main chain. On the other hand, the growth of a poly-5-ET chain can also involve homo-couplings between terminal ethynyl-functions, as well as hetero-couplings between a free  $\alpha$  position on a terminal ring and the ethynyl fragment on a second one. The presence of the unsaturated portion inside the polymer chain facilitates a more extended electron density delocalization along the polymer chain, causing the observed higher lowering of  $E_g$  values in poly-5-ET.

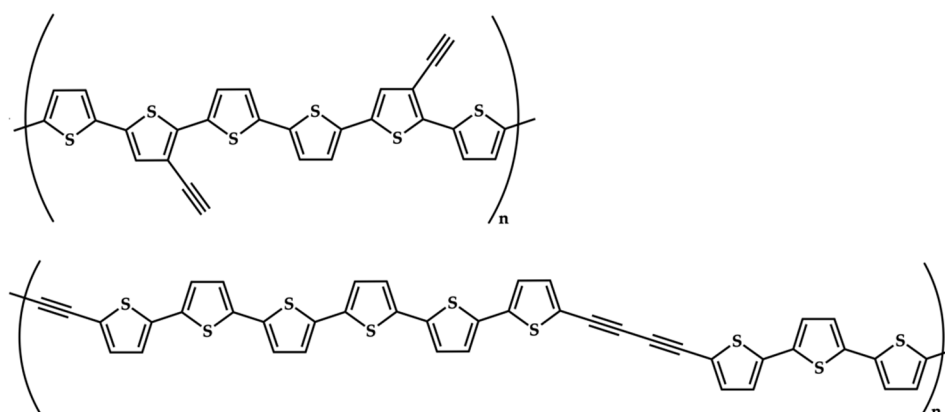


**Figure 7.** Plausible coupling of terthiophene fragments in poly-3'-ET (top) and in poly-5-ET (bottom).

#### 4. Conclusions

The effect of the nature of the substituent on a terthiophene skeleton has been investigated based on electrochemical, UV-Vis and theoretical data. In particular, 2,2':5',2''-terthiophene (2), 5-Br-terthiophene (3) and 5-ethynyl-terthiophene (5-ET), as well as the

resulting electrogenerated conducting polymers were considered. Experimental and theoretical data indicate a more extended electron density delocalization in 5-ethynyl-terthiophene, compared to both 5-Br-terthiophene and unsubstituted terthiophene. On these bases, the use of **5-ET** as the building block for highly delocalized conducting polymers can be expected to be more efficient than **2** and **3**. Such a prediction was confirmed by characterization of films obtained by electrochemical polymerization of the investigated thiophene-species. Voltammetric and UV-Vis responses evidenced a higher extended charge delocalization (expressed as  $E_g$  values) for poly-**5-ET** compared to poly-**2** and poly-**3**. Voltammetric data suggest that the lowering in  $E_g$  is mainly ascribable to a lowering in the LUMO and, in minor extension, to an increasing in the HOMO.

Finally, a comparison of 5-ethynyl-terthiophene and the resulting polymer film with the analogues reported previously, 3'-ethynyl-terthiophene (**3'-ET**) and its polymer, respectively, was performed to take into account the effect of the position of the substituent. Experimental and theoretical results again indicate a higher electron delocalization when the unsaturated fragment is located on a terminal heterocyclic ring (**5-ET**) rather than on the central one (**3'-ET**), both in the monomer and in the polymer species.

**Author Contributions:** Conceptualization, M.I.P.; methodology, M.I.P., L.M., P.M. and A.Z.; software, L.M.; formal analysis, M.I.P., E.M., L.M., P.M. and A.Z.; investigation, E.M., L.M. and P.M.; resources, M.I.P., G.S. and N.S.; writing—original draft preparation, M.I.P.; writing—review and editing, M.I.P., E.M., L.M., P.M., G.S., N.S. and A.Z.; supervision, M.I.P. and A.Z. All authors have read and agreed to the published version of the manuscript.

**Funding:** This research received no external funding.

**Institutional Review Board Statement:** Not applicable.

**Informed Consent Statement:** Not applicable.

**Data Availability Statement:** The data used in this work are available from the corresponding author on request.

**Conflicts of Interest:** The authors declare no conflict of interest. The funders had no role in the design of the study; in the collection, analyses, or interpretation of data; in the writing of the manuscript, or in the decision to publish the results.

## References

1. Dzulurnain, N.A.; Mokhtar, M.; Rashid, J.I.A.; Knight, V.F.; Wan Yunus, W.M.Z.; Ong, K.K.; Mohd Kasim, N.A.; Mohd Noor, S.A. A review on impedimetric and voltammetric analysis based on polypyrrole conducting polymers for electrochemical sensing applications. *Polymers* **2021**, *13*, 2728. [[CrossRef](#)]
2. Lu, H.; Li, X.; Lei, Q. Conjugated Conductive Polymer Materials and its Applications: A Mini-Review. *Front. Chem.* **2021**, *9*, 6–11. [[CrossRef](#)]
3. Meloni, F.; Pilo, M.I.; Sanna, G.; Spano, N.; Zucca, A. Ru(terpy)-Based Conducting Polymer in Electrochemical Biosensing of Epinephrine. *Appl. Sci.* **2021**, *11*, 2065. [[CrossRef](#)]
4. Meloni, F.; Sychalska, K.; Zając, D.; Pilo, M.I.; Zucca, A.; Cabaj, J. Application of a Thiadiazole-derivative in a Tyrosinase-based Amperometric Biosensor for Epinephrine Detection. *Electroanalysis* **2021**, *33*, 1639–1645. [[CrossRef](#)]
5. Pilo, M.; Farre, R.; Lachowicz, J.I.; Masolo, E.; Panzanelli, A.; Sanna, G.; Senes, N.; Sobral, A.; Spano, N. Design of Amperometric Biosensors for the Detection of Glucose Prepared by Immobilization of Glucose Oxidase on Conducting (Poly)Thiophene Films. *J. Anal. Methods Chem.* **2018**, *2018*, 1849439. [[CrossRef](#)]
6. Ramanavicius, S.; Ramanavicius, A. Conducting polymers in the design of biosensors and biofuel cells. *Polymers* **2021**, *13*, 49. [[CrossRef](#)]
7. Bergamini, G.; Boselli, L.; Ceroni, P.; Manca, P.; Sanna, G.; Pilo, M. Terthiophene appended with terpyridine units as receptors for Protons and  $Zn^{2+}$  ions: Photoinduced energy and electron transfer processes. *Eur. J. Inorg. Chem.* **2011**, *2011*, 4590–4595. [[CrossRef](#)]
8. Jiang, Y.; Liu, T.; Zhou, Y. Recent Advances of Synthesis, Properties, Film Fabrication Methods, Modifications of Poly(3,4-ethylenedioxythiophene), and Applications in Solution-Processed Photovoltaics. *Adv. Funct. Mater.* **2020**, *30*, 2006213. [[CrossRef](#)]
9. Logothetidis, S. Flexible organic electronic devices: Materials, process and applications. *Mater. Sci. Eng. B Solid-State Mater. Adv. Technol.* **2008**, *152*, 96–104. [[CrossRef](#)]
10. Manca, P.; Pilo, M.I.; Sanna, G.; Bergamini, G.; Ceroni, P.; Boaretto, R.; Caramori, S. Heteroleptic Ru (II)-terpyridine complex and its metal-containing conducting polymer: Synthesis and characterization. *Synth. Met.* **2015**, *200*, 109–116. [[CrossRef](#)]

11. Roncali, J. Molecular engineering of the band gap of  $\pi$ -conjugated systems: Facing technological applications. *Macromol. Rapid Commun.* **2007**, *28*, 1761–1775. [CrossRef]
12. Saito, Y.; Azechi, T.; Kitamura, T.; Hasegawa, Y.; Wada, Y.; Yanagida, S. Photo-sensitizing ruthenium complexes for solid state dye solar cells in combination with conducting polymers as hole conductors. *Coord. Chem. Rev.* **2004**, *248*, 1469–1478. [CrossRef]
13. Saranya, K.; Rameez, M.; Subramania, A. Developments in conducting polymer based counter electrodes for dye-sensitized solar cells—An overview. *Eur. Polym. J.* **2015**, *66*, 207–227. [CrossRef]
14. Hong, X.; Liu, Y.; Li, Y.; Wang, X.; Fu, J.; Wang, X. Application Progress of Polyaniline, Polypyrrole and Polythiophene in Lithium-Sulfur Batteries Xiaodong. *Polymers* **2020**, *12*, 331. [CrossRef]
15. Kondratiev, V.V.; Holze, R. Intrinsically conducting polymers and their combinations with redox-active molecules for rechargeable battery electrodes: An update. *Chem. Pap.* **2021**, *75*, 4981–5007. [CrossRef]
16. Bhosale, M.E.; Chae, S.; Kim, J.M.; Choi, J.Y. Organic small molecules and polymers as an electrode material for rechargeable lithium ion batteries. *J. Mater. Chem. A* **2018**, *6*, 19885–19911. [CrossRef]
17. Ashassi-Sorkhabi, H.; Kazempour, A. Incorporation of organic/inorganic materials into polypyrrole matrix to reinforce its anticorrosive properties for the protection of steel alloys: A review. *J. Mol. Liq.* **2020**, *309*, 113085. [CrossRef]
18. Merz, A.; Uebel, M.; Rohwerder, M. The Protection Zone: A Long-Range Corrosion Protection Mechanism around Conducting Polymer Particles in Composite Coatings: Part I. Polyaniline and Polypyrrole. *J. Electrochem. Soc.* **2019**, *166*, C304–C313. [CrossRef]
19. Riaz, U.; Nwaoha, C.; Ashraf, S.M. Recent advances in corrosion protective composite coatings based on conducting polymers and natural resource derived polymers. *Prog. Org. Coat.* **2014**, *77*, 743–756. [CrossRef]
20. Ning, C.; Zhou, Z.; Tan, G.; Zhu, Y.; Mao, C. Electroactive polymers for tissue regeneration: Developments and perspectives. *Prog. Polym. Sci.* **2018**, *81*, 144–162. [CrossRef]
21. Stejskal, J.; Sapurina, I.; Vilčáková, J.; Humpolíček, P.; Truong, T.H.; Shishov, M.A.; Trchová, M.; Kopecký, D.; Kolská, Z.; Prokeš, J.; et al. Conducting polypyrrole-coated macroporous melamine sponges: A simple toy or an advanced material? *Chem. Pap.* **2021**, *75*, 5035–5055. [CrossRef]
22. Manca, P.; Pilo, M.I.; Casu, G.; Gladiali, S.; Sanna, G.; Scanu, R.; Spano, N.; Zucca, A.; Zanardi, C.; Bagnis, D.; et al. A new terpyridine tethered polythiophene: Electrosynthesis and characterization. *J. Polym. Sci. Part A Polym. Chem.* **2011**, *49*, 3513–3523. [CrossRef]
23. Roncali, J. Conjugated Poly (thiophenes): Synthesis, Functionalization, and Applications. *Chem. Rev.* **1992**, *92*, 711–738. [CrossRef]
24. Roncali, J. Synthetic principles for bandgap control in linear  $\pi$ -conjugated systems. *Chem. Rev.* **1997**, *97*, 173–205. [CrossRef] [PubMed]
25. Roncali, J.; Garnier, F.; Lemaire, M.; Garreau, R. Poly mono-, bi- and trithiophene: Effect of oligomer chain length on the polymer properties. *Synth. Met.* **1986**, *15*, 323–331. [CrossRef]
26. Zotti, G.; Schiavon, G. Evolution of in situ conductivity of polythiophene deposits by potential cycling. *Synth. Met.* **1990**, *39*, 183–190. [CrossRef]
27. Manca, P.; Gladiali, S.; Cozzula, D.; Zucca, A.; Sanna, G.; Spano, N.; Pilo, M.I. Oligo-thiophene tethered 1,10-phenanthroline as N-chelating moiety. Electrochemical and optical characterization of the  $\pi$ -conjugated molecule and of the relevant conducting polymer and metallopolymers. *Polymer* **2015**, *56*, 123–130. [CrossRef]
28. Zanardi, C.; Scanu, R.; Pigani, L.; Pilo, M.I.; Sanna, G.; Seeber, R.; Spano, N.; Terzi, F.; Zucca, A. Synthesis and electrochemical polymerisation of 3'-functionalised terthiophenes. Electrochemical and spectroelectrochemical characterisation. *Electrochim. Acta* **2006**, *51*, 4859–4864. [CrossRef]
29. Holliday, B.J.; Swager, T.M. Conducting metallopolymers: The roles of molecular architecture and redox matching. *Chem. Commun.* **2005**, *2005*, 23–36. [CrossRef]
30. Fabrizi De Biani, F.; Reale, A.; Razzano, V.; Paolino, M.; Giuliani, G.; Donati, A.; Giorgi, G.; Mróz, W.; Piovani, D.; Botta, C.; et al. Electrochemical and optoelectronic properties of terthiophene- and bithiophene-based polybenzofulvene derivatives. *RSC Adv.* **2018**, *8*, 10836–10847. [CrossRef]
31. Hinkens, D.M.; Chen, Q.; Siddiki, M.K.; Gosztola, D.; Tapsak, M.A.; Qiao, Q.; Jeffries-El, M.; Darling, S.B. Model compounds based on poly(p-phenylenevinyleneborane) and terthiophene: Investigating the p-n junction in diblock copolymers. *Polymer* **2013**, *54*, 3510–3520. [CrossRef]
32. Zhao, X.; Piliego, C.; Kim, B.; Poulsen, D.A.; Ma, B.; Unruh, D.A.; Fréchet, J.M.J. Solution-processable crystalline platinum-acetylide oligomers with broadband absorption for photovoltaic cells. *Chem. Mater.* **2010**, *22*, 2325–2332. [CrossRef]
33. Zhu, Y.; Millet, D.B.; Wolf, M.O.; Rettig, S.J. Models for conjugated metal acetylide polymers: Ruthenium oligothiopylacetylide complexes. *Organometallics* **1999**, *18*, 1930–1938. [CrossRef]
34. Fulmer, G.R.; Miller, A.J.M.; Sherden, N.H.; Gottlieb, H.E.; Nudelman, A.; Stoltz, B.M.; Bercaw, J.E.; Goldberg, K.I. NMR chemical shifts of trace impurities: Common laboratory solvents, organics, and gases in deuterated solvents relevant to the organometallic chemist. *Organometallics* **2010**, *29*, 2176–2179. [CrossRef]
35. Hou, J.; Huo, L.; He, C.; Yang, C.; Li, Y. Synthesis and absorption spectra of poly(3-(phenylenevinyl)thiophene)s with conjugated side chains. *Macromolecules* **2006**, *39*, 594–603. [CrossRef]
36. Granovsky, A.A. Firefly Version 7.1.G. Available online: <http://classic.chem.msu.su/gran/firefly/index.html> (accessed on 16 October 2022).

37. Schmidt, M.W.; Baldrige, K.K.; Boatz, J.A.; Elbert, S.T.; Gordon, M.S.; Jensen, J.H.; Koseki, S.; Matsunaga, N.; Nguyen, K.A.; Su, S.; et al. General atomic and molecular electronic structure system. *J. Comput. Chem.* **1993**, *14*, 1347–1363. [[CrossRef](#)]
38. Perdew, J.P.; Ernzerhof, M.; Burke, K. Rationale for mixing exact exchange with density functional approximations. *J. Chem. Phys.* **1996**, *105*, 9982–9985. [[CrossRef](#)]
39. Weigend, F.; Ahlrichs, R. Balanced basis sets of split valence, triple zeta valence and quadruple zeta valence quality for H to Rn: Design and assessment of accuracy. *Phys. Chem. Chem. Phys.* **2005**, *7*, 3297–3305. [[CrossRef](#)]
40. Hohenberg, P.; Kohn, W. Inhomogeneous Electron Gas. *Phys. Rev.* **1964**, *136*, B864–B871. [[CrossRef](#)]
41. Avogadro: An Open-Source Molecular Builder and Visualization Tool. Version 1.0.3. Available online: <http://avogadro.cc/> (accessed on 16 October 2022).
42. Allouche, A. Software News and Updates Gabedit—A Graphical User Interface for Computational Chemistry Softwares. *J. Comput. Chem.* **2011**, *32*, 174–182. [[CrossRef](#)]
43. Bauerle, P.; Wurthner, F.; Gotz, G.; Effenberger, F. Selective Synthesis of  $\alpha$ -Substituted Oligothiophenes. *Synthesis* **1993**, *1993*, 1099–1103. [[CrossRef](#)]
44. Jadamiec, M.; Lapkowski, M.; Matlengiewicz, M.; Brembilla, A.; Henry, B.; Rodehüser, L. Electrochemical and spectroelectrochemical evidence of dimerization and oligomerization during the polymerization of terthiophenes. *Electrochim. Acta* **2007**, *52*, 6146–6154. [[CrossRef](#)]
45. Díaz, F.R.; Jessop, I.; Núñez, C.; Del Valle, M.A.; Zamora, P.P.; Bernède, J.C. Electrochemical synthesis of poly(3'-alkylterthiophenes). Characterization and applications. *Polym. Bull.* **2012**, *68*, 1801–1813. [[CrossRef](#)]
46. Barbarella, G.; Zambianchi, M.; Bongini, A.; Antolini, L. The Deformability of the Thiophene Ring: A Key to the Understanding of the Conformational Properties of Oligo- and Polythiophenes. *Adv. Mater.* **1993**, *5*, 834. [[CrossRef](#)]